Study of the Effect of Silver Nanoparticles Synthesized from Purslane (*Portulaca oleracea*) Extract on Liver and Kidney Functions in Mice

Mawj Ahmed Turki* , Wafaa Tali Radef, Nedhal Ibrahim Latef

Department of Biology, College of Education for Women, University of Anbar

maw23w4001@uoanbar.edu.iq

Waf-tal-1982@uoanbar.edu.iq

Edw.nedhal_79@uoanbar.edu.iq

Abstract

Plant-based silver nanoparticles (AgNPs) are emerging as adjuncts to antibiotics due to their antimicrobial and cytoprotective properties. This study evaluated AgNPs synthesized from *Purslane* (*Portulaca oleracea*) extract for hepatic and renal safety/benefit in an infection model, alone and combined with ceftriaxone (CTX) or azithromycin (AZM). Mice were allocated to seven groups: negative control (G1), bacteria only (G2), bacteria+CTX (G3), bacteria+AZM (G4), bacteria+AgNPs (G5), bacteria+CTX+AgNPs (G6), and bacteria+AZM+AgNPs (G7). Serum alanine aminotransferase (ALT), aspartate aminotransferase (AST), creatinine, and urea were measured. Liver and kidney histopathology (H&E, ×40) was assessed. One-way ANOVA with post-hoc grouping was used. Infection markedly elevated transaminases versus control (AST: 74.63 ± 6.22 vs 40.01 ± 4.14 U/L; ALT: 112.07 ± 13.65 vs 57.10 ± 4.52 U/L; both $P \leq 0.01$). Antibiotics reduced but did not normalize enzymes (G3 AST/ALT: 62.14 ± 4.71/86.23 ± 8.23 U/L; G4: 64.59 ± 6.62/88.74 ± 8.19 U/L). AgNPs alone further improved values (G5: 57.47 ± 5.69/76.02 ± 7.79 U/L). The combinations were most effective, restoring levels near control (G6: 51.82 ± 3.90/65.30 ± 5.23 U/L; G7: 51.53 ± 4.57/55.73 ± 5.09 U/L). For renal indices, infection increased urea and creatinine (58.42 ± 3.24 mg/dL; 0.714 ± 0.055 mg/dL) versus control (40.00 ± 4.19 mg/dL; 0.421 ± 0.044 mg/dL). Urea differed significantly among groups ($P = 0.0025$), while creatinine showed a nonsignificant improving trend ($P = 0.074$). Combination therapy yielded the lowest post-infection values (urea: 44.69–45.08 mg/dL; creatinine: 0.434–0.435 mg/dL), approaching control. Histologically, infection caused irregular Bowman's capsules, glomerular atrophy, tubular degeneration, inflammatory infiltration, sinusoidal dilatation, necrosis, and congestion. Antibiotics or AgNPs each attenuated these lesions; the combinations

produced kidney and liver architecture closest to normal, with only mild residual changes. AgNPs extracted by purslane enhanced the hepatic and renal outcomes of infected mice, and enhanced the action of CTX and AZM, restoring transaminases, urea and significantly improving tissue damage. These results indicate that AgNPs can be used as a bio-compatible adjuvant to antibiotics and the best effects were seen when used in combination regimens.

Keywords: **AgNPs**, Purslane (*Portulaca oleracea*), Liver, Kidney, Mice

دراسة تأثير الجسيمات النانوية الفضية المستخلصة من نبات البقلة (*Portulaca oleracea*) على وظائف الكبد والكلى في الفئران

موج أحمد تركي*، وفاء تالي ردف، نضال إبراهيم لطيف
قسم علوم الحياة، كلية التربية للبنات، جامعة الأنبار
maw23w4001@uoanbar.edu.iq
Waf-tal-1982@uoanbar.edu.iq
Edw.nedhal_79@uoanbar.edu.iq

الملخص

تُعد الجسيمات النانوية الفضية المستخلصة من النباتات (AgNPs) من المواد المكملة للمضادات الحيوية نظرًا لخواصها المضادة للميكروبات والوقائية للخلايا. هدفت هذه الدراسة إلى تقييم سلامة وفائدة AgNPs المستخلصة من نبات البقلة على الكبد والكلى في نموذج عدوى، سواء بمفردها أو بالاشتراك مع سيفترياكسون (CTX) أو أزيثروميسين (AZM). تم تقسيم الفئران إلى سبع مجموعات: التحكم السلبي (G1)، البكتيريا فقط(G2) ، البكتيريا(G3) + CTX ، البكتيريا(G4) + AZM ، البكتيريا + AgNPs (G5)، البكتيريا(G6) + CTX + AgNPs ، والبكتيريا (G7). + AZM + AgNPs تم قياس مستويات ألانين أمينوترانسفيراز(ALT) ، وأسبارتات أمينوترانسفيراز(AST) ، والكرياتينين، واليوريا في المصل. كما تم تقييم الهستولوجيا للكبد والكلى باستخدام صبغة H&E عند تكبير ×40. استخدم ANOVA أحادي الاتجاه مع تحليل بعدي للمقارنات بين المجموعات. أدت العدوى إلى ارتفاع ملحوظ في الترانسامينازات مقارنة بالتحكم (AST: 74.63 ± 6.22 مقابل 40.01 ± 4.14 وحدة/لتر؛ ALT: 112.07 ± 13.65 مقابل 57.10 ± 4.52 وحدة/لتر؛ كلاهما P≤0.01). قللت المضادات الحيوية الإنزيمات لكنها لم تعيدها للمستوى الطبيعي (G3 AST/ALT: 62.14 ± 4.71 / 86.23 ± 8.23 وحدة/لتر؛ G4: 64.59 ± 6.62 / 88.74 ± 8.19 وحدة/لتر). أدت AgNPs بمفردها إلى تحسين القيم أكثر (G5: 57.47 ± 5.69 / 76.02 ± 7.79 وحدة/لتر). كانت التركيبات المشتركة الأكثر فعالية، حيث أعادت المستويات قريبًا من التحكم (G6: 51.82 ± 3.90 / 65.30 ± 5.23 وحدة/لتر؛ G7: 51.53 ± 5.09 / 55.73 ± 4.57 وحدة/لتر. بالنسبة لمؤشرات الكلى، زادت العدوى من اليوريا والكرياتينين (58.42 ± 3.24 ملغم/دل؛ 0.714 ± 0.055 ملغم/دل) مقارنة بالتحكم (40.00 ± 4.19 ملغم/دل؛ 0.421 ± 0.044 ملغم/دل). اختلفت اليوريا بشكل معنوي بين المجموعات(P = 0.0025) ، بينما أظهر الكرياتينين اتجاه تحسني غير معنوي (P = 0.074). أظهرت المعالجة المشتركة أدنى القيم بعد العدوى (اليوريا: 44.69–45.08 ملغم/دل؛ الكرياتينين: 0.434–0.435 ملغم/دل)، مقتربة من التحكم.

هستولوجيًا، تسببت العدوى في تشوه كبسولات بومان غير منتظمة، ضمور كبيبات، تنكس أنابيب، تسلّل التهابي، توسع الجيوب، نخر واحتقان. قللت كل من المضادات الحيوية و AgNPsمن هذه التغيرات، بينما أعادت التركيبات المشتركة بنية الكبد والكلى إلى حالتها الطبيعية تقريبًا مع تغيّرات طفيفة متبقية. حسّنت AgNPsالمستخلصة من البقلة النتائج الكبدية والكلوية للفئران المصابة، وعززت تأثير CTXوAZM، مع إعادة الترانساميناز ات واليوريا وتحسين التلف النسيجي بشكل ملحوظ. تشير هذه النتائج إلى إمكانية استخدام AgNPsكعامل مكمل حيوي متوافق مع المضادات الحيوية، مع أفضل النتائج عند استخدامها في نظم علاجية مشتركة.

الكلمات المفتاحية : دقائق الفضة النانوية, نبات البقلة (*Portulaca oleracea*), الكبد, الكلى, الفئران.

1. Introduction

Plant-mediated (“green”) synthesis of silver nanoparticles (AgNPs) has gained momentum as a sustainable alternative to conventional chemical routes, leveraging phytochemicals (polyphenols, flavonoids, organic acids) as reducing and capping agents that shape nanoparticle size, morphology, and stability[1]. These green AgNPs consistently demonstrate broad antimicrobial activity and attractive biomedical potential while minimizing hazardous reagents and by-products. [2]

The antioxidant (e.g., ascorbate, carotenoids, polyphenols), bioactive plant, Portulaca oleracea (purslane) is a potent biogenic factory of AgNPs[3]. Recent studies indicate that aqueous P. oleracea extract may produce spherical AgNPs (420 nm) exhibiting a characteristic plasmon band of around 420 nm and antimicrobial/antioxidant effects, which may be very useful in the fabrication of a green nanoparticle. [4].

In addition to the intrinsic antibacterial effects, silver can be used to potentiate traditional antibiotics. Basic mechanistic experiments showed silver (and AgNP-derived Ag+) interferes with bacterial homeostasis and suppresses defenses, thereby increasing the effects of antibiotics on Gram-negative pathogens[5].

Subsequent reports—including antibiotic-loaded or co-administered AgNP systems—have confirmed synergistic or additive effects across multiple drug classes (β-lactams, macrolides, fluoroquinolones) and species, with implications for overcoming resistance and reducing required antibiotic doses. [6]

At the same time, careful **safety evaluation** is essential. AgNP exposure can produce dose-, size-, and coating-dependent hepato-renal effects in vivo, mediated by oxidative stress, inflammation, and apoptosis; conversely,

biogenic/green AgNPs may exhibit improved biocompatibility and, in some models, hepato-renal protection when appropriately dosed. These dual possibilities highlight the need for controlled dosing, rigorous biomarker monitoring, and histopathology. [7,8]

In preclinical toxicology and infection models, ALT and AST remain core serum biomarkers of hepatocellular injury, while **urea** (BUN) and **creatinine** track renal function and filtration. Elevations in ALT/AST indicate hepatocyte injury/necrosis, and changes in urea/creatinine reflect renal impairment; these markers are standard endpoints in rodent studies alongside histopathological confirmation. [9,10]

Rationale and gap. Although green-synthesized AgNPs from *P. oleracea* are promising and AgNP–antibiotic combinations show synergy, there is limited integrated evidence—within the same infection model—linking (i) serum liver/renal panels, (ii) histopathology of liver and kidney, and (iii) direct comparisons among antibiotic monotherapy, AgNP monotherapy, and **combination therapy**. Addressing this gap can clarify whether *P. oleracea*–derived AgNPs are not only effective adjuncts but also **biocompatible** at therapeutic doses.

Objective. This study investigates **silver nanoparticles biosynthesized from *P. oleracea* extract** for their impact on **liver and kidney function in infected mice**, alone and in combination with **ceftriaxone** or **azithromycin**. We quantify **ALT, AST, urea, and creatinine**, and perform **H&E histopathology** of liver and kidney to (1) determine therapeutic efficacy, (2) assess potential toxicity, and (3) evaluate synergy of AgNP–antibiotic regimens relative to monotherapies and controls.

2. Materials and methods

2.1 Key equipment

Shimadzu UV-1800 UV–Vis spectrophotometer, Olympus/Genex light microscopes, Vitek-2, autoclave, homogenizer, microtome, centrifuges, hot plate & magnetic stirrer, analytical balance, standard glassware/consumables.

2.2 Study design and animals

An in vivo controlled study was conducted (Dec-2024 to May-2025) on **35 male Swiss albino mice** (130–147 g). Animals were acclimatized 7 days under standard conditions (25 ± 2 °C; 50 ± 10% RH; 12/12 h light/dark) with ad libitum chow and sterilized water. Procedures were approved by the institutional animal ethics committee.

2.3 Experimental groups

Mice were randomized (n = 5/group) into seven groups: G1 control (non-infected), G2 bacteria only, G3 bacteria + ceftriaxone, G4 bacteria + azithromycin, G5 bacteria + AgNPs, G6 bacteria + ceftriaxone + AgNPs, G7 bacteria + azithromycin + AgNPs.

2.4 Plant extract and green AgNP synthesis

Fresh *Portulaca oleracea* was oven-dried, milled, and **50 g** powder macerated in **450 mL** absolute ethanol (homogenization 2 h; 40 °C/24 h). Filtrate was evaporated at **45 °C**; the dried extract stored at **4 °C[11]**. AgNPs: **4 g $AgNO_3$** in **100 mL** DI water (70 °C/30 min) → add **200 mL** purslane extract dropwise (stir 2 h) → hold **37 °C/48 h** → add **$NaBH_4$ (2.5 mg/mL, 10 mL)** gradually to form a dark precipitate → centrifuge, wash (water/ethanol), dry **37 °C/48 h[12]**.

2.5 Treatments and monitoring

Ceftriaxone, azithromycin and AgNPs were used according to group assignment using ready preparations of 5, 10, 15 mg/L working concentrations through IP or oral administration on fixed schedule. Clinical signs were monitored in animals on a daily basis.

2.6 Blood and tissue collection

Twenty-four hours after the final dose, mice were anesthetized (chloroform, inhalational) and blood was obtained by **cardiac puncture**. Serum was separated (4,000 rpm, 10 min; −20 °C storage).

2.7 Biochemistry

Serum **ALT, AST (U/L)** and **urea, creatinine (mg/dL)** were measured using standard assays per manufacturer instructions with routine calibration and controls.

2.8 Histopathology and IHC

Liver, kidneys, and spleen were fixed in **10% neutral-buffered formalin**, processed through graded ethanols, cleared in xylene, embedded in paraffin, sectioned at **5 µm**, and stained **H&E**. IHC used an indirect HRP-DAB method with heat-induced epitope retrieval (Tris-EDTA, pH 9.5).

2.9 Statistics

Data were analyzed by **one-way ANOVA** with appropriate post-hoc testing; significance set at **$P \leq 0.05$** (and **$P \leq 0.01$** where indicated).

3. Results And Discussion

3.1 Biochemical Analysis

3.1.1 Effect of antibiotics and silver nanoparticles on liver function and enzymes (ALT and AST) in mice

Table 1. Comparison of serum AST and ALT levels among the experimental groups.

Group	Mean ±SD	
	AST (U/L)	ALT (U/L)
G1: Negative control	D 40.01 ±4.14	D 57.10 ±4.52
G2: Bacteria only	A 74.63 ±6.22	A 112.07 ±13.65
G3: Bact.+Ceftria.	B 62.14±4.71	B 86.23 ±8.23
G4: Bacteria+Azethro.	B 64.59 ±6.62	B 88.74 ±8.19

G5: Bacteria+Nano	BC 57.47 ±5.69	BC 76.02 ±7.79
G6: Bact.+Cetr.+Nano	CD 51.82 ±3.90	C 65.30 ±5.23
G7:Bact.+Aethr.+Nano	D 51.53 ±4.57	C 55.73 ±5.09
L.S.D.	9.132**	14.124 **
P-Value	0.0011	0.0019
Means having the different letters in the same column differed significantly. ** (P≤0.01).		

CE measurements including hepatic enzymes AST and ALT had distinct, statistically differentiating results among the experimental groups ($P < 0.01$). The lowest levels were in G1 negative control 40.01 U/L 4.14 and 57.10 U/L 4.52 AST and ALT respectively, indicating normal hepatocellular structure and the lack of pathological damage. Conversely, the bacteria-only group (G2) demonstrated significant increases in both AST and ALT-74.63 + 6.22 U/L and 112.07 + 13.65 U/L, respectively- indicative of liver injury caused by bacterial infection and resulting inflammatory response, which facilitates hepatocyte lysis and enzyme release into the bloodstream, respectively.

Groups treated with antibiotics indicated significant decreases compared to bacteria-only group: G3 (ceftriaxone), 62.14 +/- 4.71 / 86.23 +/- 8.23 U/L (AST/ALT), and G4 (azithromycin), 64.59 +/- 6.62 / 88.74 +/- 8.19 U/L. Even with these reductions, values were still above the controls, which implies that, in spite of antibiotics, hepatic injuredness was partially, but not completely, reduced [14].

There was a more significant decrease in the AgNPs-only group (G5) -57.47 ± 5.69 / 76.02 ± 7.79 U/L- which suggests the presence of antimicrobial and antioxidant effects that conferred hepatoprotection, which is also consistent with the work of Hassanen et al. [15] and Yang et al. [16] that reported plant-derived silver nanoparticles enhances liver functions by minimizing inflammation, oxidative stress.

Notably, combination therapy groups showed the best post-infection outcomes: G6 (ceftriaxone + AgNPs), 51.82 + 3.90 / 65.30 + 5.23 U/L, and G7 (azithromycin + AgNPs), 51.53 + 4.57 / 55.73 + 5.09 U/L (AST/ALT), with G7 nearest to contain results. These results highlight the role of an interaction effect involving AgNPs and antibiotics: an increase in bacterial clearance and a decrease in liver toxicity; in line with Morones-Ramirez et al. [17], who demonstrated that the combination of nanoparticles and antibiotics, especially macrolides like azithromycin, enhances efficacy, decreases bacterial resistance, and results in better tissue protection.

In brief, bacterial infection resulted in overt hepatocellular damage expressed by high levels of AST and ALT, and antibiotics or AgNPs partial alleviated the damages to different extents. Combinations of these regimens were the strongest in restoring liver function indices to normal, and the two regimens in combination, azithromycin + AgNPs, should be considered synergistic, protective and curative.

Figure 1 demonstrate the (ALT) levels in study groups

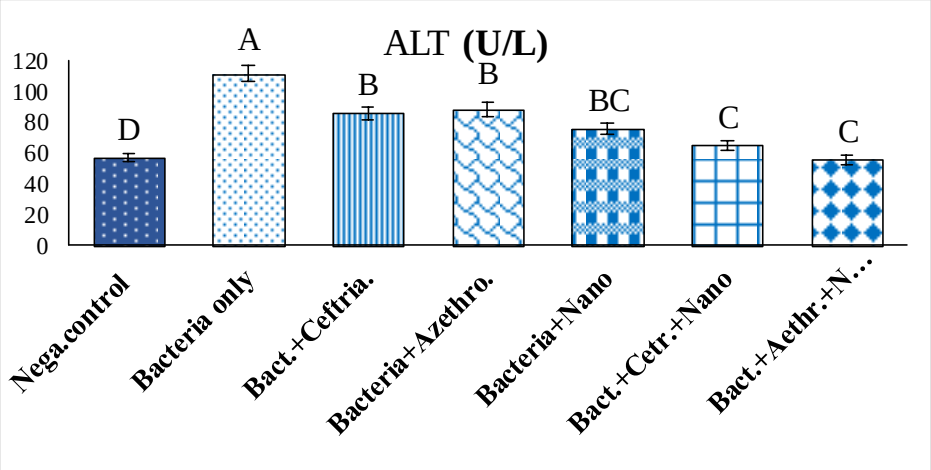

Figure 1: Effect of AgNps and antibiotics on ALT levels

Figure 2 demonstrate the (AST) levels in study groups

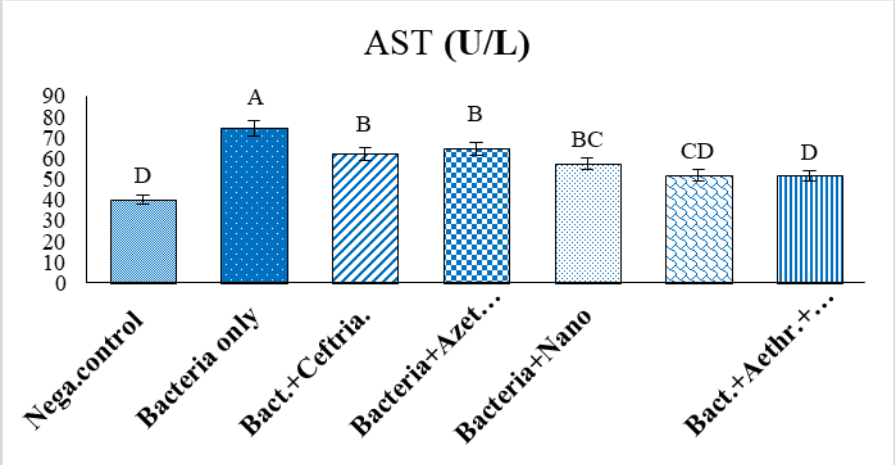

Figure 2: Effect of AgNps and antibiotics on AST levels

The two figures display the same pattern: transaminases rise with infection and improve with treatment. The bacteria-only group (G2) showed the highest values (AST = **74.63 ± 6.22 U/L**; ALT = **112.07 ± 13.65 U/L**) and was labeled **A**, whereas the negative control (G1) recorded the lowest levels (AST = **40.01 ± 4.14 U/L**; ALT = **57.10 ± 4.52 U/L**) and was labeled **D**. Monotherapy with antibiotics reduced the enzymes into the **B** range in G3 (ceftriaxone) and G4 (azithromycin), though still above control. Silver nanoparticles alone (G5) produced a further decrease to **BC** (AST ≈ **57.5 ± 5.7 U/L**; ALT ≈ **76.0 ± 7.8 U/L**). The combination regimens performed best after the control: G6 (ceftriaxone + nano) reached **CD** for AST and **C** for ALT (AST = **51.82 ± 3.90 U/L**; ALT = **65.30 ± 5.23 U/L**), while G7 (azithromycin + nano) was **D** for AST—i.e., not significantly different from control—and **C** for ALT (AST = **51.53 ± 4.57 U/L**; ALT = **55.73 ± 5.09 U/L**). Letters above the bars indicate groups that are not significantly different when they share the same letter and are significantly different when letters differ (ANOVA; AST: P = **0.0011**, ALT: P = **0.0019**). In general, the results indicate that the synergistic effect between silver nanoparticles and antibiotics (particularly, azithromycin) yields a more significant effect on reducing AST/ALT to physiological levels, thereby preventing infection-related hepatic damage.

Bars represent mean ± SD.

3.1.2 Effect of antibiotics and silver nanoparticles on renal function (creatinine and urea) in mice

Table 2. Comparison of serum creatinine and urea concentrations among the experimental groups.

Group	Mean ±SD	
	Creatinine mg/dL	Urea mg/dL
G1: Negative control	C 0.421 ±0.044	D 40.00 ±4.190
G2: Bacteria only	A 0.714 ±0.055	A 58.42 ±3.237
G3: Bact.+Ceftria.	B 0.505 ±0.029	B 50.86 ±2.377
G4: Bacteria+Azethro.	B 0.488 ±0.025	BC 49.70 ±4.864
G5: Bacteria+Nano	B 0.482±0.042	BCD 49.84 ±4.145
G6: Bact.+Cetr.+Nano	BC 0.435 ±0.018	CD 44.69±5.006
G7:Bact.+Aethr.+Nano	BC 0.434±0.030	CD 45.08±0.865
L.S.D.	6.630 *	0.064 **
P-Value	0.074	0.0025
Means having the different letters in the same column differed significantly. ** (P≤0.01).		

The serum creatinine and urea measurements showed some differences among the experimental groups. G1 was the lowest (creatinine: 0.421 + 0.044 mg/dL; urea: 40.00 + 4.19 mg/dL), which is typical of normal renal physiology. Conversely, the bacteria-only G2 group indicated significant increases (creatinine: 0.714 + 0.055 mg/dL; urea: 58.42 + 3.24 mg/dL) compared to control suggesting that infection causes renal dysfunction due to inflammation and oxidative stress,

which have been discussed in recent studies relating systemic infections to increased kidney damage markers.[18,19].

In the antibiotic-treated groups (G3: ceftriaxone; G4: azithromycin), values declined relative to G2—**creatinine ~0.505–0.488 mg/dL** and **urea ~50.86–49.70 mg/dL**—indicating partial improvement due to bacterial inhibition; however, levels remained above control, which may be related to antibiotic-associated renal effects with continued use [20].

The AgNPs group (G5) showed a similar improvement (**creatinine: 0.482 ± 0.042 mg/dL; urea: 49.84 ± 4.14 mg/dL**), supporting the notion that AgNPs mitigated renal damage via antimicrobial and antioxidant actions, as reported by Fan et al..[21] Notably, the combination therapies (G6: CTX+Nano; G7: AZM+Nano) were the most effective, with values approaching control (**creatinine ~0.43–0.44 mg/dL; urea ~44.69–45.08 mg/dL**). This indicates a synergistic effect between AgNPs and antibiotics, enhancing therapeutic efficacy and reducing infection-related renal injury; recent findings likewise show that nanoparticle–antibiotic combinations improve treatment performance and protect vital organs, including the kidney [22].

Taken together, bacterial infection caused a clear disturbance in renal function indices, whereas the **combined** antibiotic–AgNP regimens were the most efficient in restoring values toward normal, underscoring the importance of a synergistic approach to renal protection during infection.

Figure 3 demonstrate the (Urea) levels in study groups

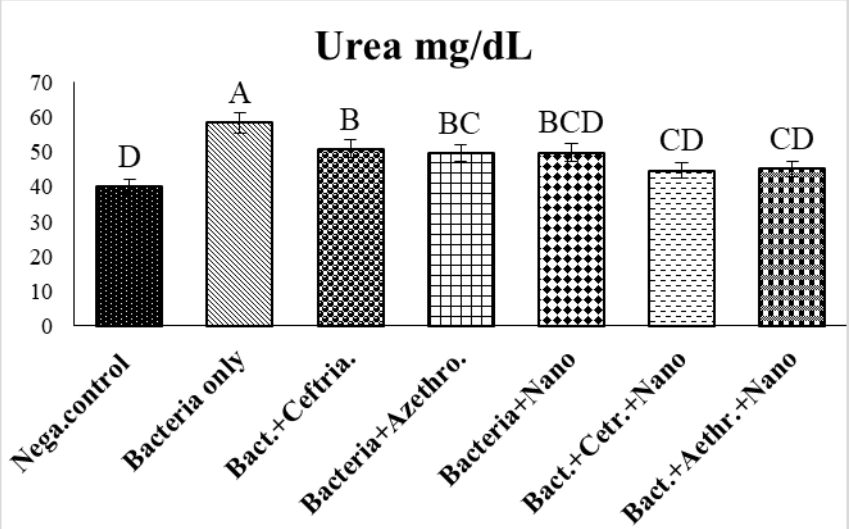

Figure 3: Effect of AgNps and antibiotics on Urea levels

Figure 4 demonstrate the (Creatinine) levels in study groups

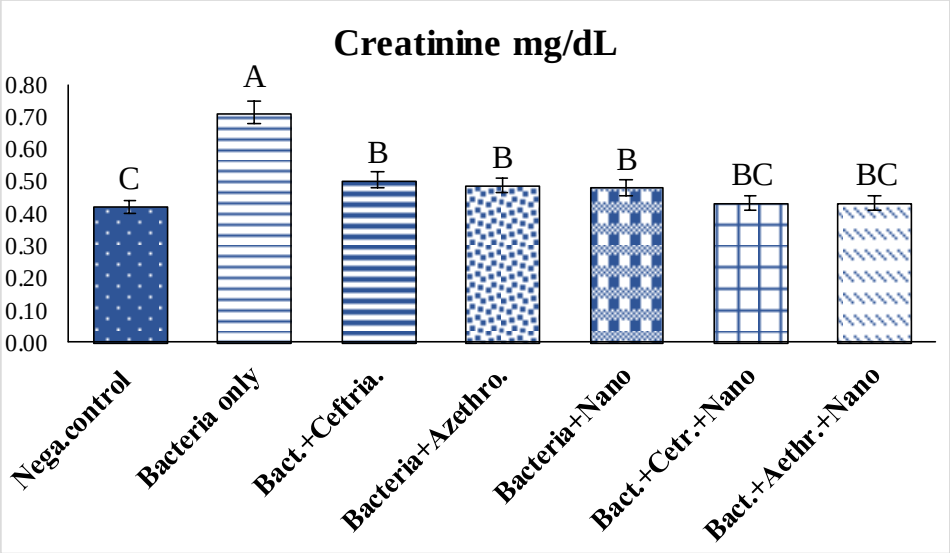

Figure 4: Effect of AgNps and antibiotics on creatinine levels

The two graphs depict a steady rise in renal failure due to infection and a progressive improvement on therapy. In the case of urea, the groups distinguished themselves (ANOVA, P = 0.0025): the G2 group, which consisted of bacteria alone, registered the highest (58.42 ± 3.24mg/dL, letter A), whereas no other group had the lowest (40.00 ± 4.19mg/dL, D) value.

Monotherapy with antibiotics reduced urea to **B** in **G3** (50.86 ± 2.38) and to **BC** in **G4** (49.70 ± 4.86), while silver nanoparticles alone **G5** (49.84 ± 4.15) yielded **BCD**. The **combination regimens** showed the best improvement after the

control, with **G6 (**CTX + Nano) **and** G7 (AZM + Nano) **approaching normal values (**44.69 ± 5.01 **and** 45.08 ± 0.87 mg/dL**, letter** CD).

For **creatinine**, infection produced a clear rise **(**G2: 0.714 ± 0.055 mg/dL**,** A) compared with control (G1: 0.421 ± 0.044 mg/dL**,** C**).** Values decreased with antibiotic monotherapy (G3: 0.505 ± 0.029; G4: 0.488 ± 0.025 mg/dL**, both** B) and with AgNPs alone (**G5: 0.482 ± 0.042**, **B**). The lowest values occurred with the **combined treatments** (G6: 0.435 ± 0.018; G7: 0.434 ± 0.030 mg/dL**,** BC). Despite this favorable trend, the overall comparison was not statistically significant (ANOVA, *P* = **0.074**), so letter-based differences should be interpreted cautiously.

Letters above the bars indicate groups that are **not significantly different** when they share the same letter and **significantly different** when the letters differ. In general, the infection increased both urea and creatinine, and the entire treatments reduced these increases, with the combination treatments (CTX/AZM + AgNPs) (particularly AZM + AgNPs) returning values to control, indicating a synergistic nephroprotective effect. (Bars represent mean ± SD.)

3.2 **Histopathology Study**

3.2.1 Mice Kidney Histology

The kidney fragments showed an evident gradient of lesion severity in accordance with the treatment received:

Negative control (G1; Figure 5): Bowman normal appearance; normal glomeruli (GL) without inflammatory renal infiltration/fibrosis/congestion; normal cortical tubules (CT) in order with patent lumina and intact epithelial lining- normal histological control.

• Bacteria alone (G2; Figure 6): Abnormal Bowman capsule (IBC) and glomerular tuft atrophy (AGL), with intense mononuclear cell infiltration (IM), vascular congestion (CO) and severe degenerative alterations in cortical tubules (DCT)- are consistent with vigorous inflammatory and oxidative stress responses and impaired glomerular filtration efficiency.

• Ceftriaxone alone (G3; Figure 7) and azithromycin alone (G4; Figure 8): Some improvement compared to G2; no severe shrinkage of glomerular tufts with no severe infiltration and no severe tubular degeneration, suggesting infection control without full restoration of the normal architecture.

• Silver nanoparticles only (G5; Figure 9): Improvement is more significant; slight glomerular atrophy, slight infiltrate, slight tubular changes, come closer to the physiological image compared to antibiotic monotherapy.

• Combination therapy- G6 (ceftriaxone + AgNPs; Figure 10) and G7 (azithromycin + AgNPs; Figure 11): Approach normal morphology; normal BC, GL with slight shrinkage, limited IM, and slight DCT changes. These results suggest that AgNPs synergize with antibiotics (reduced inflammatory infiltration and congestion and maintained renal architecture).

Overall severity ranking:

G2 (worseest) > G3 ≈ G4 > G5 > G6 ≈ G7 ≈ G1 (nearest to normal).

This concordant finding of these histological observations is consistent with renal function biomarkers (urea/creatinine) with the combination regimens (CTX/AZM + AgNPs) approximating control values, and the combined solution (CTX/AZM + AgNPs) was likely to play a protective-therapeutic role in limiting the renal injury caused by infection.

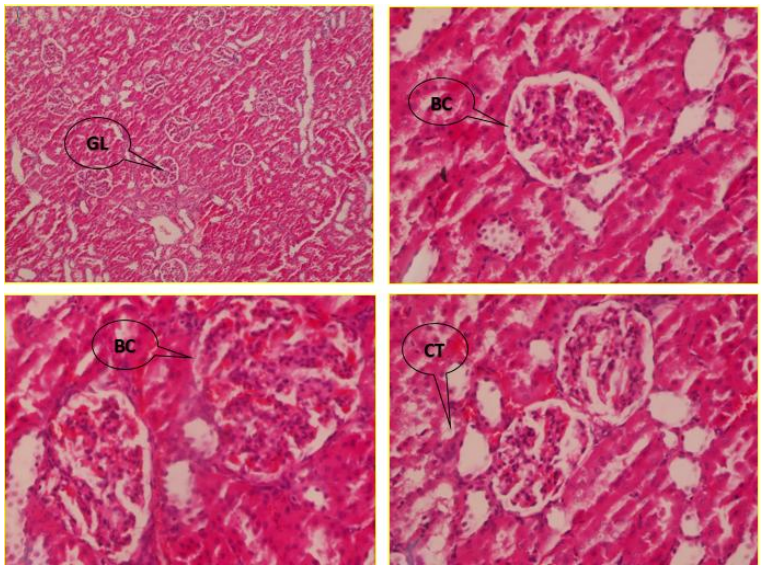

Print ISSN 2710-0952 Electronic ISSN2790-1254

Figure (5):- Histopathological section of Kidney control group show: Normal Bowman capsule (BC), Normal glomeruli (GL), Normal cortical tubules (CT), (H and E stain) ,(40X).

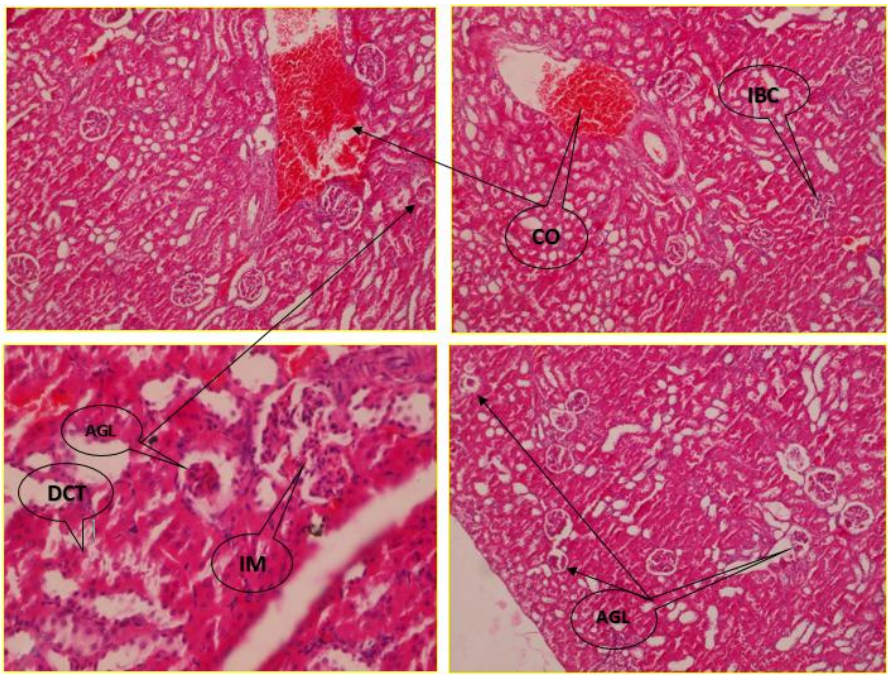

Figure (6):- Histopathological section of Kidney positive control group show: Irregular Bowman capsule (IBC), Atrophy in glomeruli tuft (AGL), heavy infiltration of mononuclear cells (IM) severe degenerative changes in the cortical tubules (DCT), congestion (CO), (H and E stain) ,(40X).

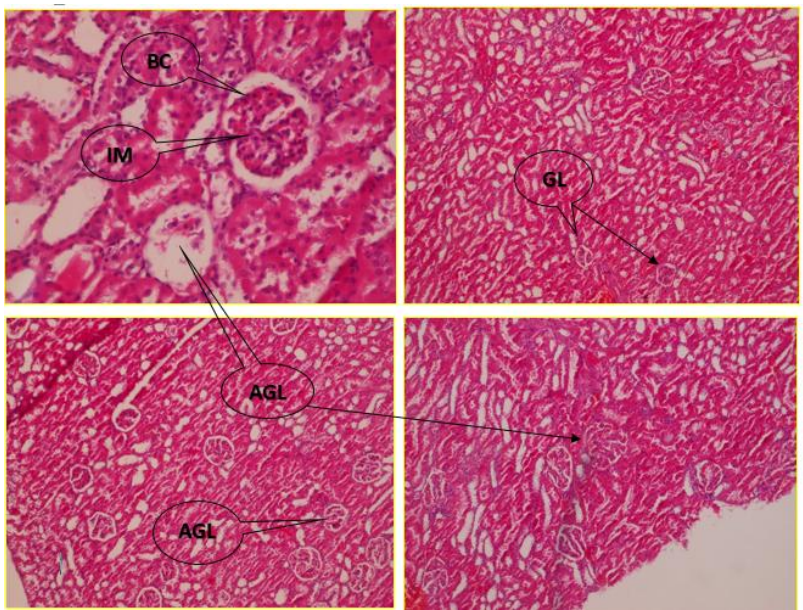

Figure (7):- Histopathological section of Kidney (G3) group show: Normal Bowman capsule (BC), moderate shrinkage in glomeruli tuft (GL), moderate infiltration of mononuclear cells (IM) moderate degenerative changes in the cortical tubules (DCT), (H and E stain) ,(40X).

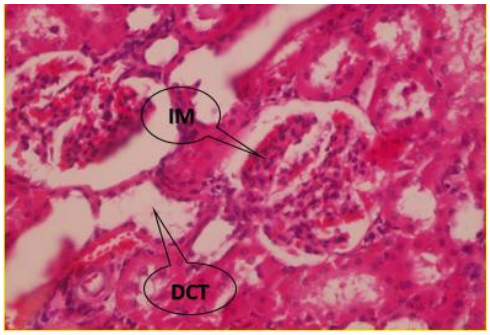

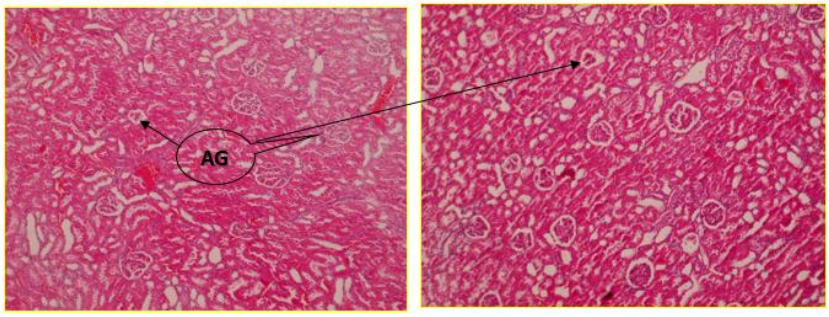

Figure (8):- Histopathological section of Kidney (G4) group show: Normal Bowman capsule (BC), moderate shrinkage in glomeruli tuft (GL), moderate infiltration of mononuclear cells (IM) moderate degenerative changes in the cortical tubules (DCT), (H and E stain) ,(40X).

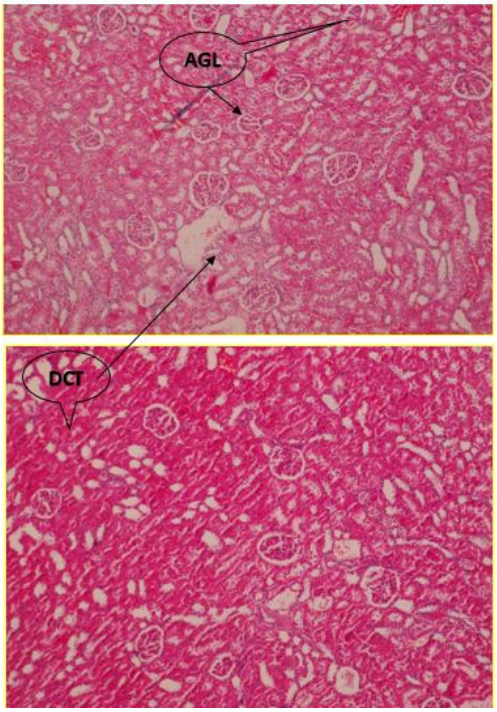

Figure (9):- Histopathological section of Kidney (G5) group show: Normal Bowman capsule (BC), mild shrinkage in glomeruli tuft (GL), mild infiltration of mononuclear cells (IM) mild degenerative changes in the cortical tubules (DCT), (H and E stain) ,(40X).

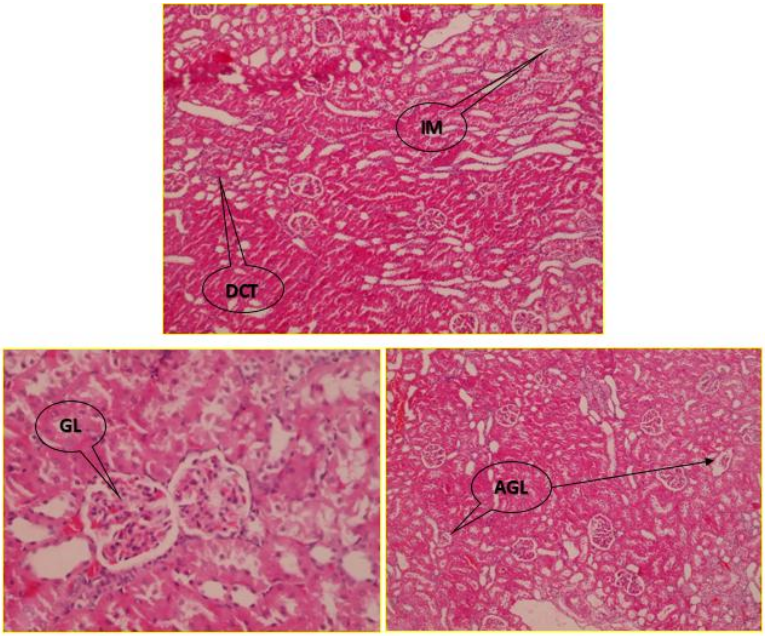

Figure (10):- Histopathological section of Kidney (G6) group show: Normal Bowman capsule (BC), mild shrinkage in glomeruli tuft (GL), mild infiltration of mononuclear cells (IM) mild degenerative changes in the cortical tubules (DCT), (H and E stain) ,(40X).

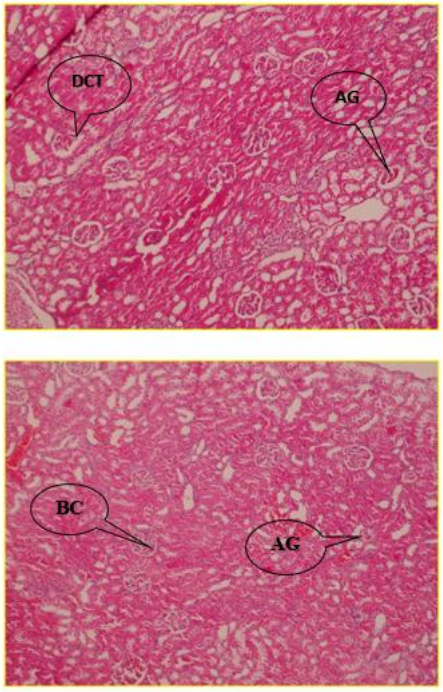

Figure (29-4):Histopathological section of Kidney (G7) group shows: Normal Bowman capsule (BC), mild shrinkage in glomerular tuft (GL), mild infiltration of mononuclear cells (IM), mild degenerative changes in the cortical tubules (DCT), (H and E stain),(40X).

3.2.2. Liver histology

The liver sections exhibited a clear gradient of lesion severity that paralleled the treatment modality:

- Negative control (G1; Figure 12): Normal hepatic architecture; hepatocytes (HC) radiating around the central vein (CV), sinusoidal spaces (SS) regular, and a normal portal triad without inflammatory infiltration or

necrosis. This micrograph serves as the normal histological reference for comparison.

- Bacteria only (G2; Figure 13): Overt injury characterized by parenchymal hypertrophy (PH), sinusoidal dilatation (dSS), and moderate mononuclear inflammatory infiltration (IC), with necrotic foci (NC) and vascular congestion (CO)—indicating an inflammation- and oxidative stress–driven architectural disturbance.
- Ceftriaxone alone (G3; Figure 14): Partial improvement; a quasi-normal architecture with mild hepatocellular hypertrophy, reduced SS caliber, limited infiltration, and small scattered necrotic foci.
- Azithromycin alone (G4; Figure 15): A quasi-normal picture similar to G3, with mild hypertrophy, limited infiltration, and a slight reduction in SS; necrosis and congestion were less prominent than in G3.
- Silver nanoparticles alone (G5; Figure 16): More pronounced improvement; near-normal architecture with orderly hepatic plates around the CV, moderate and uniform SS, moderate hypertrophy in some cells, and limited infiltration, without extensive necrosis.
- Combination therapy (G6: ceftriaxone + AgNPs; Figure 17) and (G7: azithromycin + AgNPs; Figure 18): A clearly near-normal architecture; orderly radial plates around the CV, clear and regular SS, only mild hypertrophy, and minimal infiltration, with no notable necrosis. These findings reflect a synergistic effect between AgNPs and antibiotics, reducing inflammation and congestion and preserving hepatic architecture.

Overall severity ranking:G2 (most severe) > G3 ≈ G4 > G5 > G6 ≈ G7 ≈ G1 (closest to normal).These observations are consistent with ALT/AST profiles: infection was associated with marked elevations, whereas all treatments produced a stepwise decline. The combined regimens (CTX/AZM + AgNPs) most effectively restored both architecture and enzyme values toward physiological limits, supporting synergistically enhanced hepatoprotection.

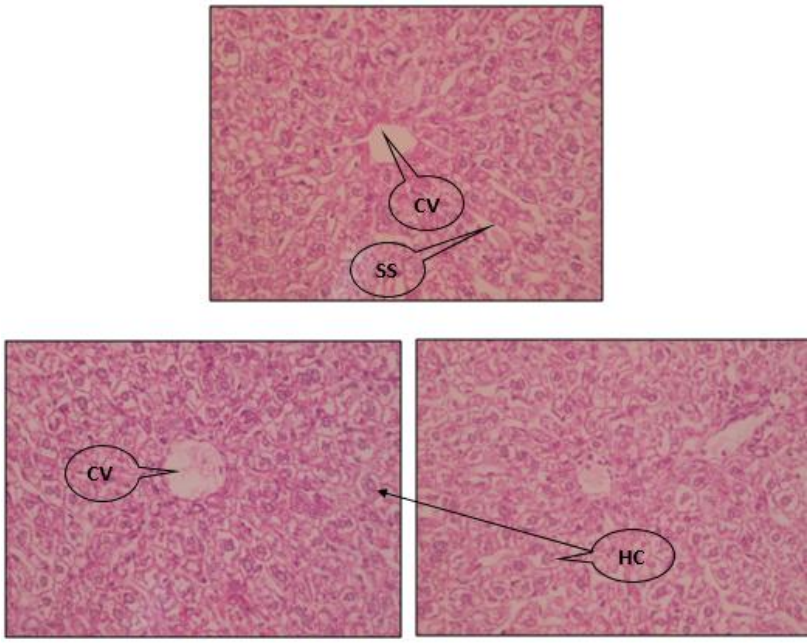

Figure (12):- Histopathology of rat liver control rats group: show normal architecture of the liver with hepatocytes (HC) radiating from the central vein (CV), sinusoidal space (SS) and portal triad, Optic microscopy: H&E (×40).

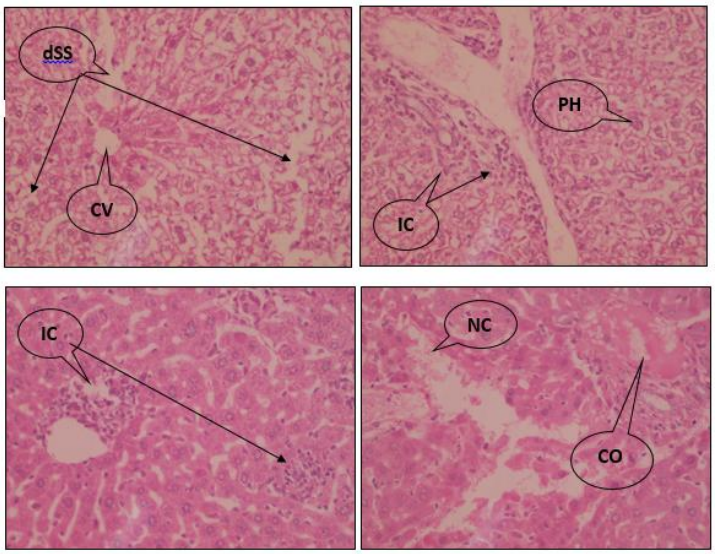

Figure (13):- Histopathology of rat liver Bacteria treated rats group: show moderate parenchymal cells hypertrophy (PH), dilatation of sinusoidal space (dSS) with mild inflammatory cell infiltration (IC), Necrosis (NC), congestion (CO), Optic microscopy: H&E (×40).

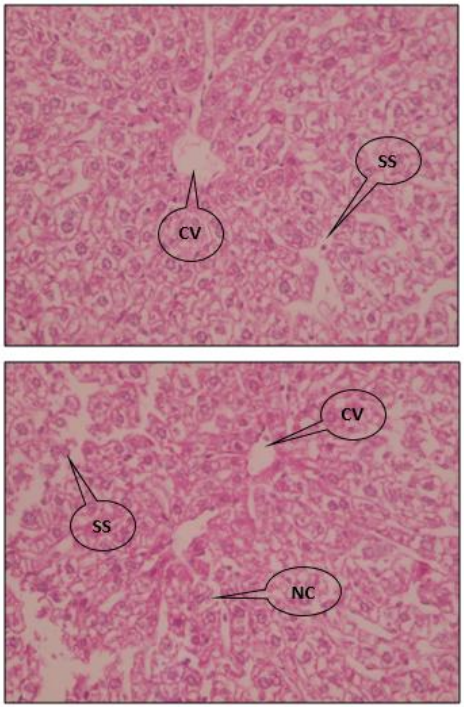

Figure (14):- Histopathology of rat liver (G3) rats group: show normal architecture of the liver with hepatocytes (HC) radiating from the central vein (CV), mild parenchymal cells hypertrophy, reduction in sinusoidal space (SS) and inflammatory cell infiltration, Optic microscopy: H&E (×40).

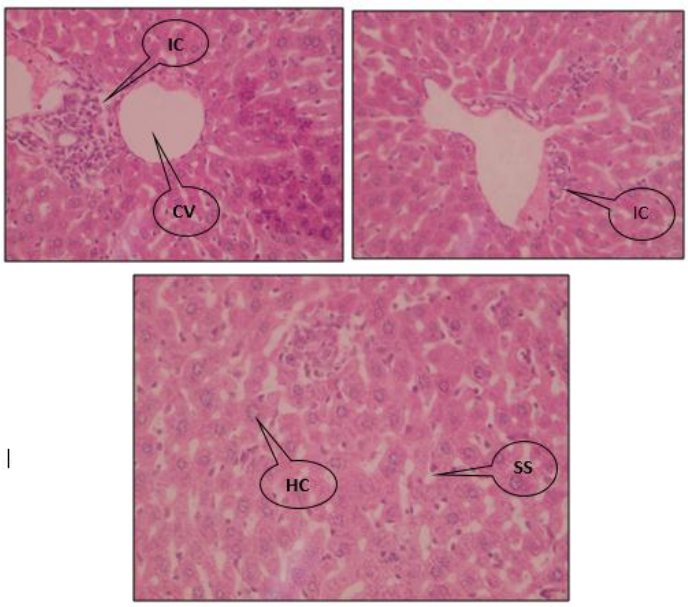

Print ISSN 2710-0952 Electronic ISSN2790-1254

Figure (15):- Histopathology of rat liver (G4) rats group: show normal architecture of the liver with hepatocytes (HC) radiating from the central vein (CV), mild parenchymal cells hypertrophy, reduction in sinusoidal space (SS) and inflammatory cell infiltration, Optic microscopy: H&E (×40).

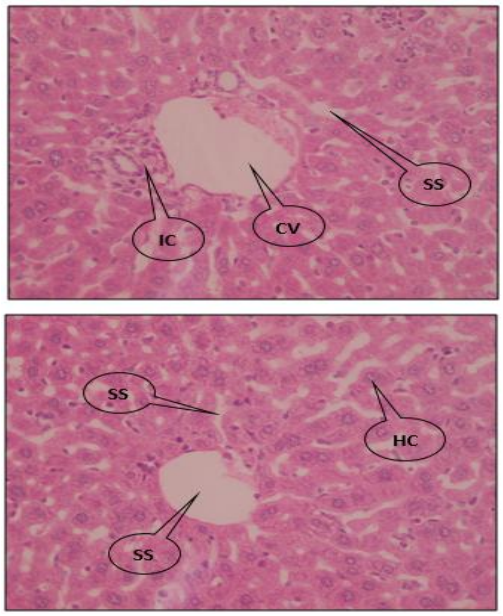

Figure (16):- Histopathology of rat liver (G5) rats group: show normal architecture of the liver with hepatocytes (HC) radiating from the central vein (CV), Moderate parenchymal cells hypertrophy, reduction in sinusoidal space (SS) and inflammatory cell infiltration, Optic microscopy: H&E (×40).

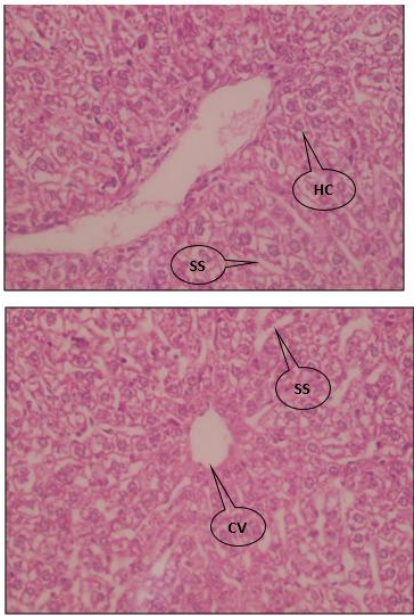

Figure (17):- Histopathology of rat liver (G6) rats group: show normal architecture of the liver with hepatocytes (HC) radiating from the central vein (CV), Moderate parenchymal cells hypertrophy, reduction in sinusoidal space (SS) and inflammatory cell infiltration, Optic microscopy: H&E (×40).

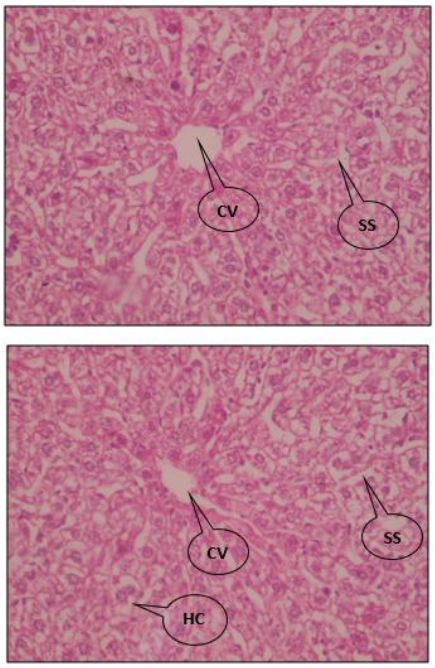

Figure (18):- Histopathology of rat liver (G7) rats group: show normal architecture of the liver with hepatocytes (HC) radiating from the central vein (CV), Moderate parenchymal cells hypertrophy, reduction in sinusoidal space (SS) and inflammatory cell infiltration, Optic microscopy: H&E (×40).

4. Conclusion

In summary, bacterial infection elicited pronounced hepatic and renal injury, reflected by elevated serum AST/ALT and urea/creatinine and corroborated by severe histopathological changes. Antibiotic monotherapies (ceftriaxone or azithromycin) attenuated but did not normalize these abnormalities, whereas silver nanoparticles (AgNPs) alone produced greater biochemical and architectural recovery. The greatest improvement occurred with the combination regimens (ceftriaxone+AgNPs or azithromycin+AgNPs), which returned indices closest to control values (AST and ALT: P = 0.0011 and 0.0019; urea: P = 0.0025), with creatinine showing a concordant, though nonsignificant, trend (P = 0.074); notably, azithromycin+AgNPs rendered AST values indistinguishable from controls. The histology of the liver and kidneys reflected these patterns, showing a progression from significant injury in infected animals to nearly normal architecture with the use of combination therapy. The data collectively suggest a synergistic interaction between AgNPs and antibiotics that enhances antibacterial efficacy and reduces inflammation and oxidative stress-related organ damage, highlighting AgNPs as a promising adjuvant to conventional treatment.

References

1. Firdhouse, M. J., & Lalitha, P. (2012). Green synthesis of silver nanoparticles using the aqueous extract of Portulaca oleracea (L.). *Asian Journal of Pharmaceutical and Clinical Research*, *6*(1), 92-94.
2. Al-Otibi, F., Alfuzan, S. A., Alharbi, R. I., Al-Askar, A. A., Al-Otaibi, R. M., Al Subaie, H. F., & Moubayed, N. M. (2022). Comparative study of antifungal activity of two preparations of green silver nanoparticles from Portulaca oleracea extract. *Saudi Journal of Biological Sciences*, *29*(4), 2772-2781.
3. Fouda, A., Al-Otaibi, W. A., Saber, T., AlMotwaa, S. M., Alshallash, K. S., Elhady, M., ... & Abdel-Rahman, M. A. (2022). Antimicrobial, antiviral, and in-vitro cytotoxicity and mosquitocidal activities of Portulaca oleracea-based green synthesis of selenium nanoparticles. *Journal of Functional Biomaterials*, *13*(3), 157.
4. Aboulthana, W. M., Omar, N. I., Hasan, E. A., Ahmed, K. A., & Youssef, A. M. (2022). Assessment of the biological activities of Egyptian purslane (Portulaca oleracea) extract after incorporating metal nanoparticles, in vitro and in vivo study. *Asian Pacific Journal of Cancer Prevention: APJCP*, *23*(1), 287.
5. Abdel-Rahman, M. A., Alshallash, K. S., Eid, A. M., Hassan, S. E. D., Salih, M., Hamza, M. F., & Fouda, A. (2024). Exploring the antimicrobial,

antioxidant, and antiviral potential of eco-friendly synthesized silver nanoparticles using leaf aqueous extract of Portulaca oleracea L. *Pharmaceuticals*, *17*(3), 317.

6. Iziy, E., Majd, A., Vaezi-Kakhki, M. R., Nejadsattari, T., & Noureini, S. K. (2019). Effects of zinc oxide nanoparticles on enzymatic and nonenzymatic antioxidant content, germination, and biochemical and ultrastructural cell characteristics of Portulaca oleracea L. *Acta Soc. Bot. Pol*, *88*(4), 3639.
7. Amirazodi, E., Zaman, M., Khanchoupan, M., Moghadam, F. M., Faravani, F., Abolfazl, A. K., & Jafarianmoghadam, N. (2024). Therapeutic Potential of ZnO-Nanoparticles Synthesized Using Portulaca oleracea in Cancer Treatment: A Comprehensive Narrative Review. *Research in Biotechnology and Environmental Science*, *3*(4), 46-53.
8. Lee, Y. J., & Park, Y. (2020). Graphene oxide grafted gold nanoparticles and silver/silver chloride nanoparticles green-synthesized by a Portulaca oleracea extract: Assessment of catalytic activity. *Colloids and Surfaces A: Physicochemical and Engineering Aspects*, *607*, 125527.
9. Barzinjy, A. A., & Haji, B. S. (2024). Green synthesis and characterization of Ag nanoparticles using fresh and dry Portulaca Oleracea leaf extracts: Enhancing light reflectivity properties of ITO glass. *Micro & Nano Letters*, *19*(3), e12198.
10. Ahn, E. Y., Lee, Y. J., Park, J., Chun, P., & Park, Y. (2018). Antioxidant potential of Artemisia capillaris, Portulaca oleracea, and Prunella vulgaris extracts for biofabrication of gold nanoparticles and cytotoxicity assessment. *Nanoscale Research Letters*, *13*(1), 348.
11. S. Naz et al., “Therapeutic potential of selected medicinal plant extracts against multi-drug-resistant *Salmonella enterica* serovar Typhi,” Saudi Journal of Biological Sciences, vol. 29, no. 2, pp. 941–954, Feb. 2022.
12. A. Tariq et al., “Restraining the multidrug efflux transporter STY4874 of Salmonella Typhi by reserpine and plant extracts,” Letters in Applied Microbiology, vol. 69, no. 3, pp. 161–167, Sep. 2019.
13. Dong, J., Wang, T., Li, H., Zhang, J., Zhang, H., Liu, W., ... & Fu, Q. (2023). Polyphenol-based antibacterial and antioxidative nanoparticles for improved peritonitis therapy. *Collagen and Leather*, *5*(1), 34.
14. Yin, H., Zhou, M., Chen, X., Wan, T. F., Jin, L., Rao, S. S., ... & Xie, H. (2021). Fructose-coated Ångstrom silver prevents sepsis by killing bacteria and attenuating bacterial toxin-induced injuries. *Theranostics*, *11*(17), 8152.

15. Hassanen, E. I., & Ragab, E. (2021). In vivo and in vitro assessments of the antibacterial potential of chitosan-silver nanocomposite against methicillin-resistant Staphylococcus aureus–induced infection in rats. *Biological Trace Element Research*, *199*(1), 244-257.

16.Yang, N., Wu, T., Li, M., Hu, X., Ma, R., Jiang, W., ... & Zhu, C. (2025). Silver-quercetin-loaded honeycomb-like Ti-based interface combats infection-triggered excessive inflammation via specific bactericidal and macrophage reprogramming. *Bioactive materials*, *43*, 48-66.

17. Morones-Ramirez, J. R., Winkler, J. A., Spina, C. S., & Collins, J. J. (2013). Silver enhances antibiotic activity against gram-negative bacteria. *Science translational medicine*, *5*(190), 190ra81-190ra81.

18. Ayipo, Y. O., Badeggi, U. M., Jimoh, A. A., & Mordi, M. N. (2024). Silver nanoparticles for treatment of COVID-19 and other viral diseases. In *Silver Nanoparticles for Drug Delivery* (pp. 313-340). Academic Press.

19. Takallu, S., Mirzaei, E., Zakeri Bazmandeh, A., Ghaderi Jafarbeigloo, H. R., & Khorshidi, H. (2024). Addressing antimicrobial properties in guided tissue/bone regeneration membrane: enhancing effectiveness in periodontitis treatment. *ACS Infectious Diseases*, *10*(3), 779-807.

20. Wang, Y., Zhang, M., Yan, Z., Ji, S., Xiao, S., & Gao, J. (2024). Metal nanoparticle hybrid hydrogels: the state-of-the-art of combining hard and soft materials to promote wound healing. *Theranostics*, *14*(4), 1534.

21. Fan, W., Han, H., Chen, Y., Zhang, X., Gao, Y., Li, S., ... & Yao, K. (2021). Antimicrobial nanomedicine for ocular bacterial and fungal infection. *Drug Delivery and Translational Research*, *11*(4), 1352-1375.

22. Facal Marina, P., Kaul, L., Mischer, N., & Richter, K. (2022). Metal-Based Nanoparticles for Biofilm Treatment and Infection Control: From Basic Research to Clinical Translation. *Antibiofilm Strategies: Current and Future Applications to Prevent, Control and Eradicate Biofilms*, 467-500.